

# ISTITUTO NAZIONALE DI FISICA NUCLEARE

Sezione di Trieste

---

**INFN/TC-89/4**

**14 luglio 1989**

A. Barbiellini, P. Bregant, E. Castelli, P. Ciuti, L. Dalla Palma, R. Giacomich,  
G. Gozzi, F. de Guarrini, A. Penzo, P.G. Rancoita, A. Rindi, F. Stacul,  
G. Tromba, and S. Vitale

**STATUS REPORT ON:**

**THE USE OF SYNCHROTRON RADIATION IN DIGITAL  
MAMMOGRAPHY**



**STATUS REPORT ON:  
THE USE OF SYNCHROTRON RADIATION  
IN DIGITAL MAMMOGRAPHY**

**A. Barbiellini, E. Castelli, P. Ciuti, R. Giacomich and A. Penzo**  
Dipartimento di Fisica Università di Trieste and Sezione INFN di Trieste,

**P. Bregant and F. de Guarini**  
Servizio di Fisica Sanitaria and USL N. 1 Triestina

**G. Gozzi, L. Dalla Palma and F. Stacul**  
Istituto di Radiologia Università di Trieste

**P.G. Rancoita**  
Sezione INFN di Milano

**A. Rindi and G. Tromba**  
Sincrotrone Trieste and Sezione INFN di Trieste

**S. Vitale**  
Sezione INFN di Genova



## 1. - Introduction

The increasing number of synchrotron light sources (SLS) has produced an intense renewed interest in the application of low-energy photon beams in many scientific and technical domains.

Photon beams of energy 10-100 keV (X-ray beams) obtained from SLS can have interesting applications in medicine owing to the characteristic properties of the SLS X-Ray beams: monochromaticity, high intensity and good collimation.

Previous internal reports [1], [2] have been devoted to a feasibility study of the applications of synchrotron radiation (SR) from the Trieste facility to digital subtraction angiography (SYRDA). However, the SYRDA programs at DESY, Stanford and Tsukuba [3], are already oriented towards high-intensity beams, which could be achieved also at the Trieste facility only using multipole wigglers configurations with high magnetic field.

X-ray mammography ([4], [5], [6], [7]) is another very interesting field of application for synchrotron radiation.

In this paper, after some clinical considerations about the current request for mammography, we examine the use of the monochromatized S.R. beam in mammography, where the problems of motion artifacts are less critical and consequently a lower beam intensity is required.

Compared with conventional sources, it will be shown that the intense, tunable X-ray spectrum of a SR facility allows considerable improvements in the quality of the images, in terms of contrast and spatial resolution for the same absorbed dose to the patient.

In addition, the use of thin strip detectors like the solid state Si strip commonly used in high energy physics research, can add some substantial improvements to the detected image. For this peculiarity we present, also, some preliminary results of measurements of the efficiency of a solid state Si detector to low energy radiations.

## 2. - Clinical considerations.

The medical community is in general agreement with the concept that an early detection of breast cancer affects the prognosis of the patients: they survive longer and, sometimes, totally recover. That is why breast cancer screening programs, initially introduced as research projects (M.I.P. - Health Insurance Plan - BCDDP - Breast Cancer Detection Demonstration Project), became a definite diffuse reality with the aim of detecting malignancies as soon as possible in asymptomatic women. Screening procedures can be defined as periodic control of an apparently healthy population to achieve an early

(\*) The sensitivity is defined as the ratio between the number of successful diagnosis on the total number of examinations.

The radiation from a conventional diagnostic X-ray tube used in mammography covers the energy range between 10 and 30 keV (fig.1), the size of the radiation field is approximately  $18 \times 24 \text{ cm}^2$  and the exposure times are in the range between a few tenths of

### 3. - Characteristics of an SLS X-ray beam. Comparison with the conventional sources.

In the appendix we review the historical evolution of mammography.

mammographic findings.

However ultrasonography usually follows mammography and takes benefit of

74% for lesions smaller than 2 cm.

Ultrasonographic sensitivity is between 75% and 90%; these values is reduced to 67%-

nature of a focal lesion.

mammography when the latter is limited by a dense breast or is unable of assessing the however in the great majority of cases it is a second step procedure, following Ultrasonography is the first procedure in symptomatic young females (under 35); consequent significant improvement of image quality and therefore of its diagnostic value. Ultrasonography recently underwent a quick technological development, with a

91%.

diagnosis varies between 80% and 95%; in lesions smaller than 2 cm it is around 88- Recently a consistent technological improvement was achieved (units with grids, new detectors, possibility of magnification,...). Mammographic sensitivity(\*) in cancer

and of occult neoplasms in the contralateral breast.

lesion, its size and extent to deep tissues, the presence of other non palpable neoplasms node is discovered, because it is possible to define the benign or malignant nature of the screening; the procedure is performed in symptomatic patients as well, when a breast Mammography has been and presently is the main examination in breast cancer

should undergo screening tests every 2 years.

examinations are to be performed yearly, as each woman between the age of 40 and 70

Females within the Trieste district are about 130000; therefore 20000-25000 mammary

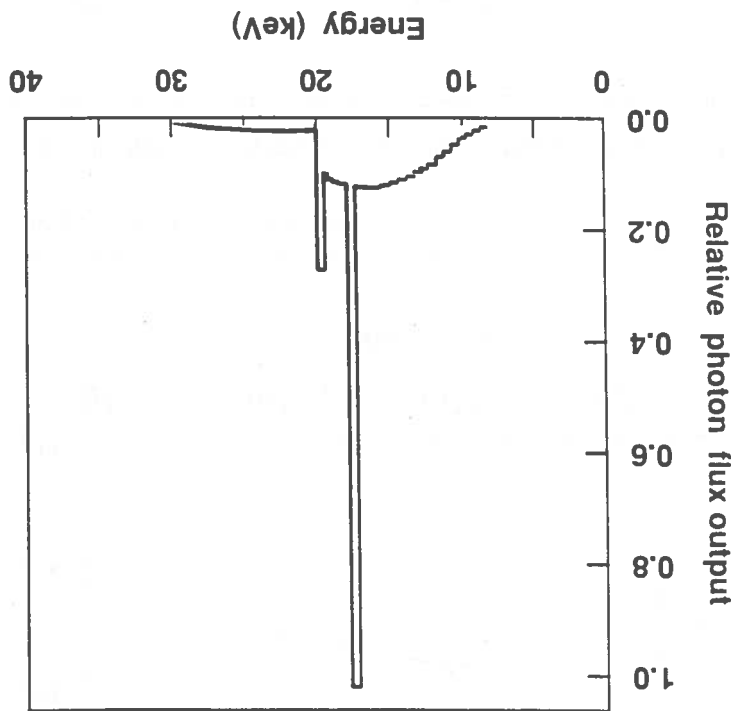
doubling time of a neoplasm.

diagnosis. Interval follow-ups of 1.5-2 years are suggested, on the basis of the mean

In this kind of examinations the absorbed dose at a thickness of 3 cm lies in the range between 0.18 mSv and 0.83 mSv in radiographies using intensifying screens and between 2.3 mSv and 5.5 mSv in xeromammography [4].

On the other hand, a typical SR spectrum (fig.2) obtained from a wavelength shifter in a 2 GeV ring with a circulating average current of 200 mA gives a flux density of about  $7 \times 10^{12}$  photons/(mrad s 0.1% bandwidth) at 20 keV in a laminar beam of 0.25 mrad of vertical angular opening. This corresponds to a flux of about  $10^{11}$  photons/(mm<sup>2</sup>s) in a bandwidth of 20 eV for a beamline length of 15 m.

Fig. 1 : A typical X-ray spectrum from a conventional tube as used in mammography. Voltage = 30kV, molybdenum 17° target, Filters: 1 mm Beryllium + 0.03 mm molybdenum.



a second to a few seconds, depending on the involved depths, since the flux at 20 keV is about  $10^6$  photons/(mm<sup>2</sup> s) at 75 cm from the source. The energy spectrum is wide, with a peak corresponding to the characteristic X-ray energy of the target, generally Molybdenum.

the cut of most of the scattered radiation. In addition, a reduction of the absorbed dose by using a monochromatic beam is assured since the useless low energy component present in the conventional X-ray spectrum is eliminated. Also, an improvement in contrast resolution is expectable from X-ray beam as a function of the depth, as it will be shown in the next section.

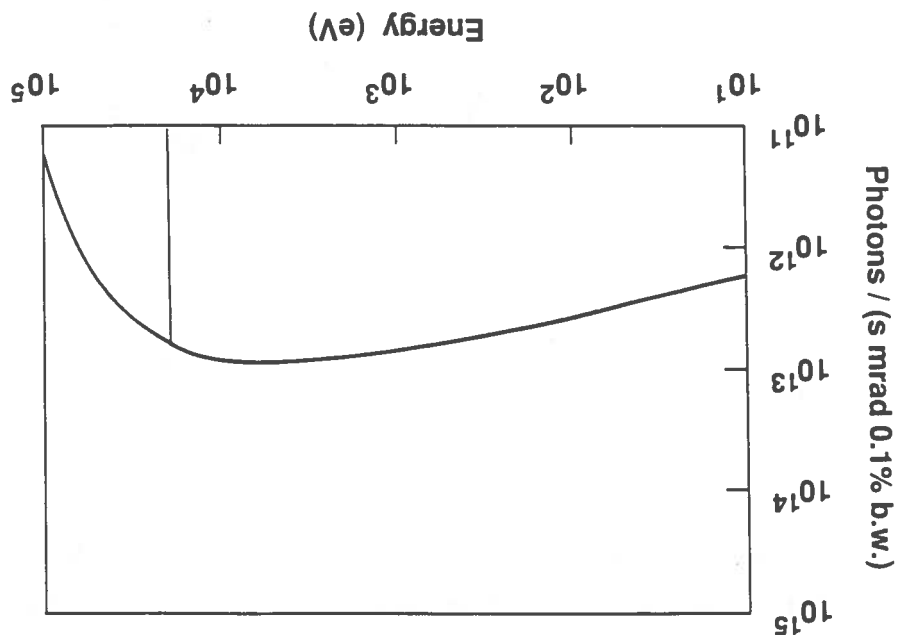
Moreover, the use of monochromatic SR beams allows to optimize the energy of the scanning of the region to be investigated. Using SR laminar beams coupled with one-dimensional detectors it will be possible to eliminate most of the diffused radiation which is scattered also at large angles. Of course, in such a geometry the patient must be moved through the beam to have a complete scanning of the region to be investigated.

The scattered radiation generated in Compton and Rayleigh interactions is detrimental to the imaging: it reduces the contrast of the image and causes blurring.

The purpose of radiodiagnosis in general is to evidence objects of a given composition from an environment of different composition by the detection of the transmitted X-rays. This is possible if the two media absorb the X-ray radiation differently. Ideally, only X-ray interactions that cause the absorption of the X quantum (photoelectric effect) are useful.

At these energies the attenuation of the beam in the patient is due to three mechanisms: photoelectric absorption, inelastic (or Compton) scattering, elastic (or Rayleigh) scattering.

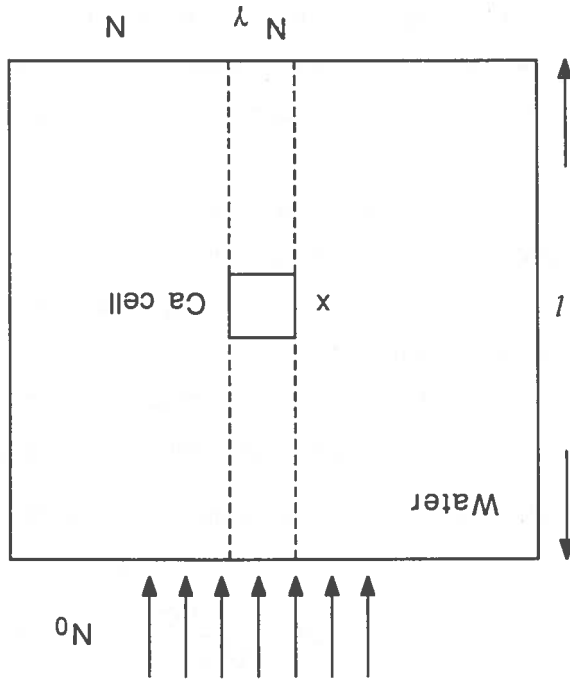
Fig. 2 : X-ray spectrum from a wavelength shifter of an electron storage ring. Beam energy = 2 GeV, Current = 200 mA, magnetic field in the shifter = 7 T.





It is easy to show that for given dimensions of the water-box and Ca cell there is an energy of the X-ray beam which optimizes the information.

Fig. 3 : The geometry considered the calculation of the optimization parameter.



For a preliminary theoretical prevision of the optimization of the beam energy, we have considered a box full of water (simulating the tissue), containing a small Ca cell (simulating the calcification) whose density is much higher than density of water (fig.3).

More than in other types of radiological imaging, in mammography, two limit cases can be considered: the detection of very small structures (i.e. a volume of about  $1 \text{ mm}^3$ ) in a medium whose absorption coefficient is much different from the coefficient of the investigated structure and the imaging of larger size objects in a low contrast background. The first case characterizes the space resolution, the second one the resolution in contrast. For instance, one of the goals of mammography is to detect the presence and the dimensions of microcalcifications which often suggest a malignant tumor.

**4 - Optimization of the beam energy: theoretical forecast.**

Finally, exposure times, and consequently motion artifacts, can be reduced since SR flux is much higher.

Let us indicate by:

- $l$  = water box depth;
- $x$  = Ca cell dimension along the direction of  $l$ ;
- $\mu_1$  = water attenuation coefficient;
- $\mu_2$  = Ca attenuation coefficient;
- $N_0$  = number of incident photons per  $\text{cm}^2$  of the box (fluence);
- $N$  = number of particles transmitted per  $\text{cm}^2$  through water only;
- $N\gamma$  = number of particles transmitted per  $\text{cm}^2$  through water and Ca;
- $E$  = energy of photons.

If the contribution of the scattered radiation can be neglected, it results:

$$N = N_0 e^{-\mu_1 l}$$

$$N\gamma = N_0 e^{-\mu_1(l-x)} e^{-\mu_2 x}$$

We define as "optimization parameter" (O.P.) the ratio:

$$\frac{D}{N_0} = \frac{N_0}{(N - N\gamma)} = e^{-\mu_1 l} (1 - e^{-(\mu_2 - \mu_1)x})$$

In fact,  $\frac{D}{N_0}$  indicates the relative value of the effective signal detected.

The figs. 4a and 4b show some plots of this parameter as a function of the energy for different values of  $l$  and  $x$ . It is evident that there is a value of  $E$  which maximizes the optimization parameter, even if there are no K-edge absorption energies in this range. For instance, for values of  $l = 5$  cm and  $x = 0.1$  cm, the optimum energy lies between 30 keV and 35 keV, which is rather far from the energy peak of a conventional X-ray tube. The errors drawn in the figure are due to the errors on the values of the X-ray absorption cross sections.

These considerations are valid if the fluence  $N_0$  of the monochromatic beam is known and if unidimensional detectors are used to minimize the scattered radiation.

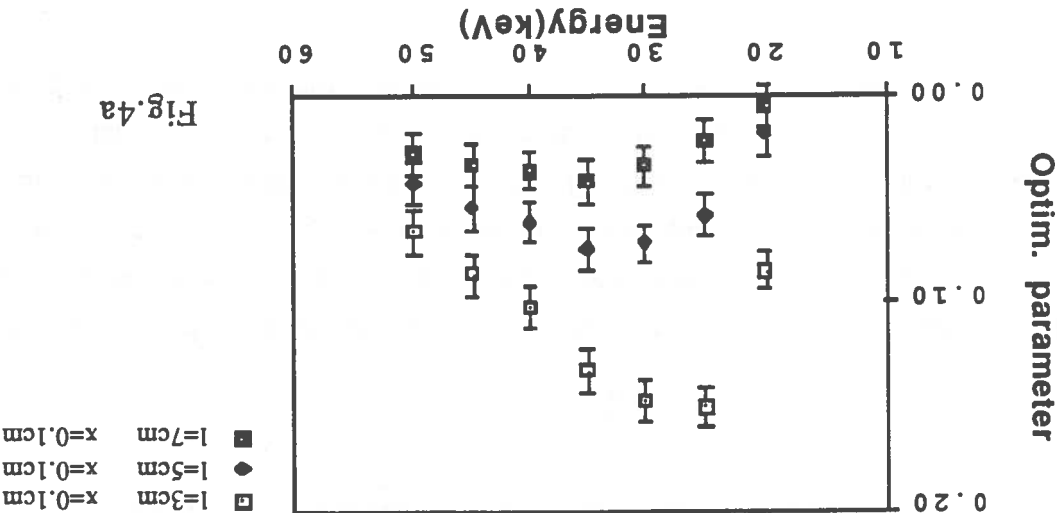
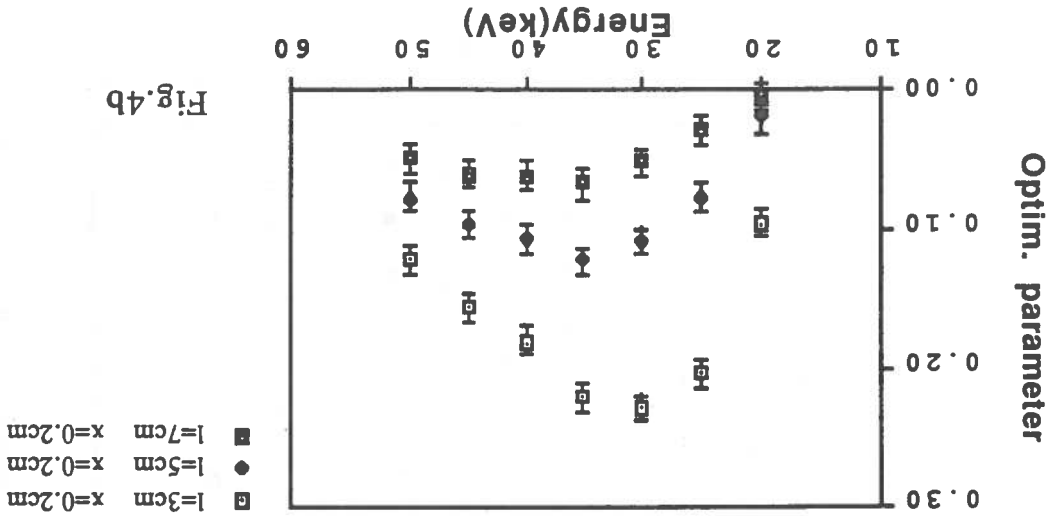
We are performing, also, a more accurate study of the optimization using a Montecarlo simulation program which takes into consideration all the photon interactions including Compton and Rayleigh scattering.

We evaluate the minimum fluence requested in each of the two cases. In the first case, to be able to detect the presence of the microcalcification, the value of  $N_g$  must be statistically different from  $N$ . If  $\sqrt{N}$  is the standard deviation on  $N$ , the relation :  $D = k \sqrt{N}$  gives the significance of our test as a function of the number of standard deviations  $k$ .

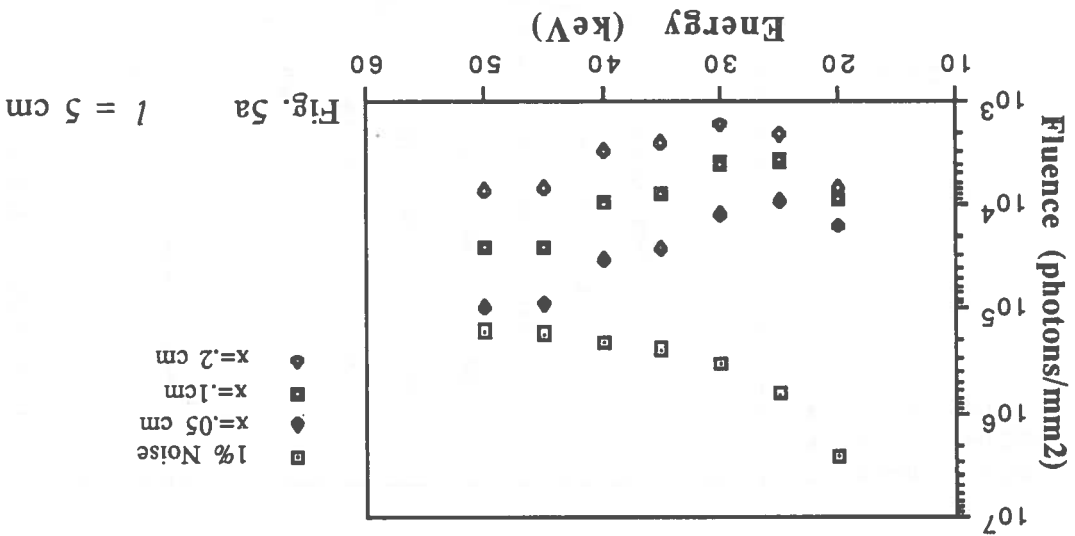
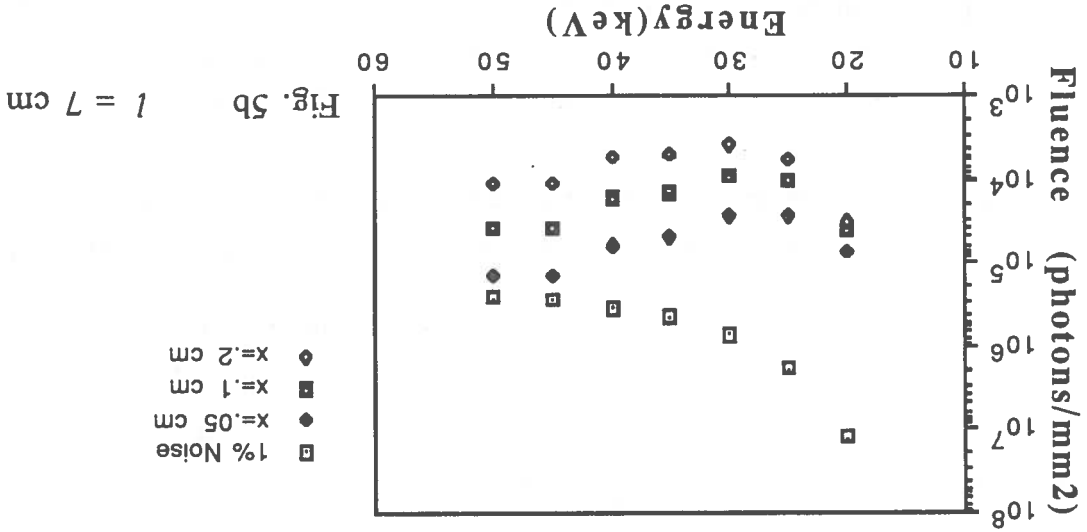
- ii) the request for an image of clinical quality.
  - "yes/no");
  - i) the check of the existence of the microcalcification (which gives an information type
- In the detection of the microcalcification, we can distinguish two goals:

5. - Experimental requirements.

Figs 4a and 4b : Plots of the optimization parameter  $\frac{D}{N_0}$  as a function of the X-ray energy E for different values of  $l$  and  $x$ .



Figs. 5a and 5b : The fluence  $N_0$  requested to detect the presence of a Ca cell in a water matrix as a function of the X-ray energy  $E$  for different values of the thickness of the Ca cell  $x$  and of the water depth  $l$  with a statistical factor of 5.



The figs. 5a and 5b show the values of the minimum fluence requested to detect the presence of the Ca cell as a function of  $E$  for different values of  $l$  and  $x$ , for  $k=5$ . In the second case, for having an image of clinical quality, it is necessary to set an absolute value of the statistical noise per pixel. For instance, we can require to have the 1% of the statistical noise outside of the region interested by the Ca cell. These two cases lead to different requirements for the fluence as shown in figs. 5a and 5b.

$$N_0 = \frac{(1 - e^{-(\mu_2 - \mu_1)x})^2}{k^2 e^{\mu_1 l}}$$

Given  $k$ , we obtain the minimum value of  $N_0$  which fulfil our needs:

Water area	50 x 50 mm <sup>2</sup>
Strip width	0.9 mm
Gap between the strips	0.1 mm
Water resistivity	2.0 k $\Omega$ cm
Depletion voltage	60 V
Dark current at 60 V	20 nA
Capacity per strip at 60V	40 pF

Following characteristics:

Meanwhile some tests have been carried out using an existing Si strip detector with the has been despatched in September 1988. The constructive design of this counter has been realized and calls for tender have been sent out. Two leading manufacturers of Si detectors, Hamamatsu and Micron Semiconductor, are ready to produce a prototype counter at reasonable cost. The order in 1987 [3].

A preliminary project has been presented at the SYRDA meeting held at Frascati of the type described in refs [8], [9], [10], with high efficiency optimized for such a attention also to the theoretical and experimental study of a solid state X-ray detector Beyond the theoretical approach presented in sections 4 and 5, we have devoted our

## 6. - X-ray detector.

In the configuration of the Trieste facility which will run at 2 GeV of energy, 400 mA of current, out of the bending magnet of 1.2 T the flux density at 35 keV and at 15 m distance from the source will be approximately of  $3 \times 10^8$  photons/(mm<sup>2</sup>s) in a bandwidth of 1%. This is well adequate for a very short time exposure. good quality image.

In such a condition, one can calculate a surface dose of about  $8 \times 10^{-2}$  mSv for taking a

- detection efficiency of 75%.
  - monodimensional array of detectors having sizes of  $0.5 \times 0.5$  mm<sup>2</sup> or lower; thickness);
  - flux of about  $1 \times 10^8$  photons/(s mm<sup>2</sup>) at 35 keV in the worst geometry (7 cm of - monochromatic beams in the energy range between 25 keV and 35 keV;
- for a medical beamline devoted to digital mammography are:
- Assuming an exposure time of 10 ms for each scan, the experimental requirements These fluence must be obtained for each scan.

electronics has been neglected. 5b. In both calculations, the detection efficiency has been set to 75% and the noise due to

The dashed peak which appears around the 26<sup>th</sup> - strip may be attributed to some Ortec model 570.

The electronic chain is a commercial one: preamplifier Silena model 205, amplifier was not collimated. In the measurement the polarization voltage  $V_p$  has been set equal to 50 V and the source Figure 7 shows the ratio of the full width at half maximum (FWHM) to the peak channel, versus the strip number. This quantity gives the energy resolution of each strip.

Fig.6: The peak channel of the pulse-height distribution for a particle on a strip versus the strip number.

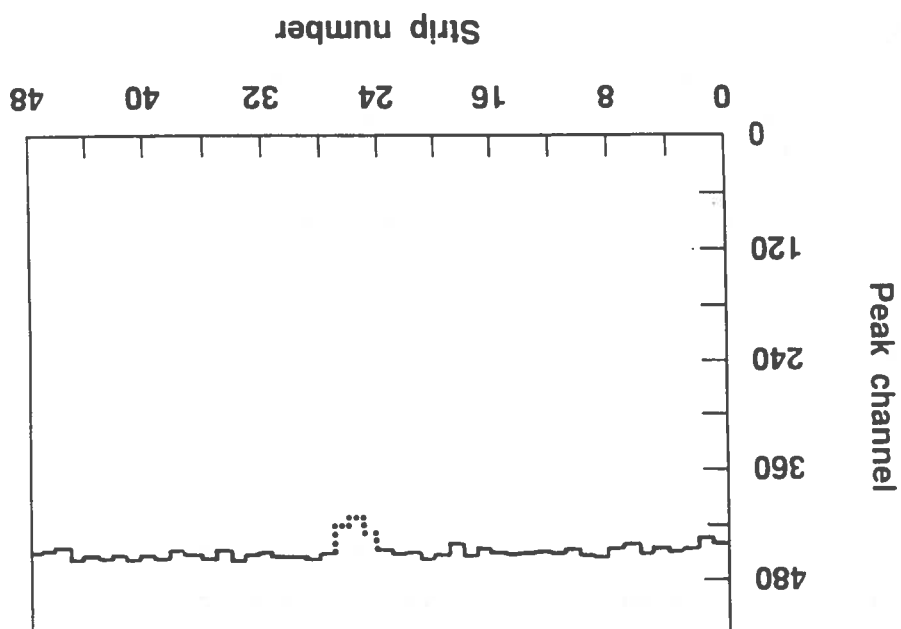


Figure 6 shows the peak channel of the pulse-height distribution of the response of each strip to the  $\alpha$ -particle from  $^{241}\text{Am}$ , versus the strip number.

7.1 - Exposure to  $\alpha$ -source.

## 7. - Experimental results

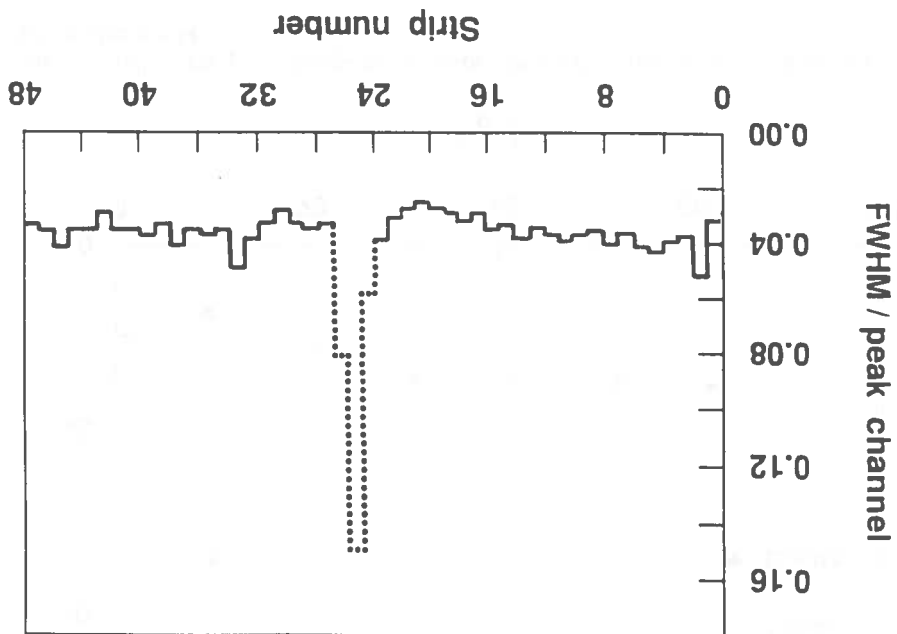
The response of the detector has been investigated with the following sources:  $\alpha$ -source  $^{241}\text{Am}$  ( $E = 5.476 \text{ MeV}$ ),  $\beta$ -sources  $^{106}\text{Ru}$  ( $E = 0.874 \text{ MeV}$ ) and  $^{90}\text{Sr}$  ( $E = 2.274 \text{ MeV}$ ), characteristic X-rays sources from Mo ( $E = 17.4 \text{ keV}$  and  $19.6 \text{ keV}$ ), Ag ( $E = 22.1 \text{ keV}$  and  $25.0 \text{ keV}$ ), Ba ( $E = 32.1 \text{ keV}$  and  $36.6 \text{ keV}$ ), Tl ( $E = 44.2 \text{ keV}$  and  $50.6 \text{ keV}$ ) and  $\gamma$ -source Am ( $E = 59.5 \text{ keV}$ ). In the last two cases the photons strike the detector strip both from a direction perpendicular and parallel to the detection layer.

dispersion is about 50 keV. The measure of the dispersion introduced by the electronic chain is shown in fig. 10. In the figure the pulse-height distribution obtained using test pulses of the same amplitude of the pulses from  $\beta$ -particles is shown versus the channel number. The value of the

The ratio of the FWHM to the peak channel number of the pulse height distributions considered are shown in fig. 9 as a function of  $V_p$ . The ratio of a test beam at CERN (crosses). For comparison in the figure are reported also the results obtained by high energy  $^{90}\text{Sr}$  sources. The peak channel of the pulse height distribution obtained using the  $^{106}\text{Ru}$  source (white circles) and the  $^{90}\text{Sr}$  source (dark circles) as a function of  $V_p$  are shown in fig. 8. We determined the response of the detector as a function of  $V_p$  using the  $^{106}\text{Ru}$  and by the  $\beta$ -particle.

The response of the detector is analyzed when a coincidence occurs between the strip and a detector beyond the strip. This condition guarantees the full crossing of the detector 7.2 - Exposure to  $\beta$ -source.

Fig. 7 : The ratio of the FWHM to the peak channel versus the strip number for  $\alpha$  particles; polarization voltage = 50 V.



damaged strips. The dark-current intensity of the damaged strips was higher than the current intensity values of the good ones.

Fig. 9: The ratio of the FWHM to the peak channel number as a function of the polarization voltage for  $\beta$  particles.

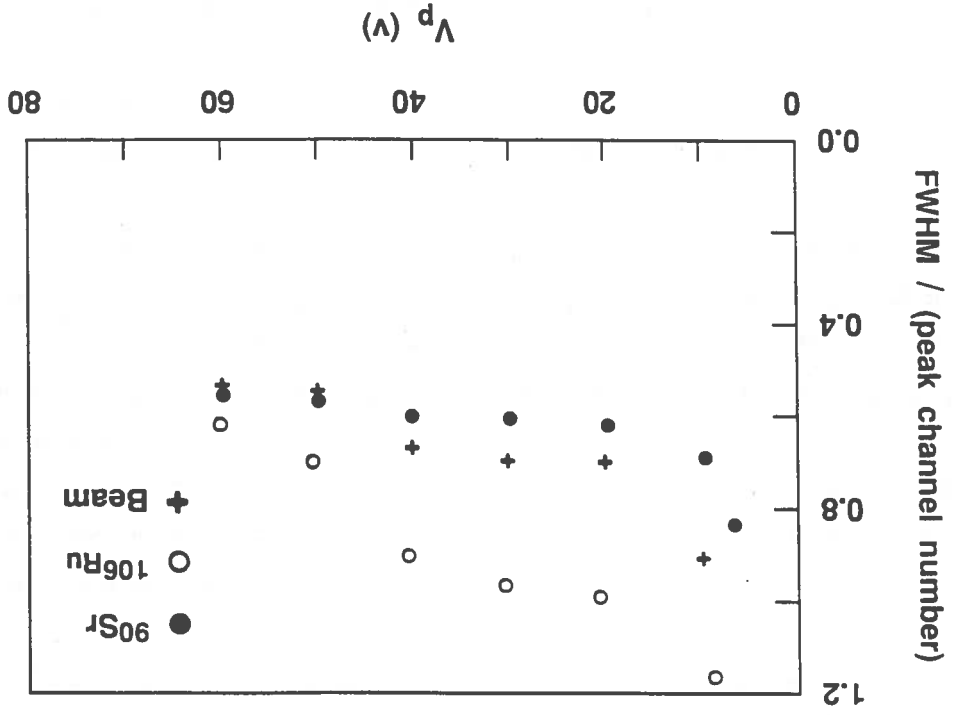
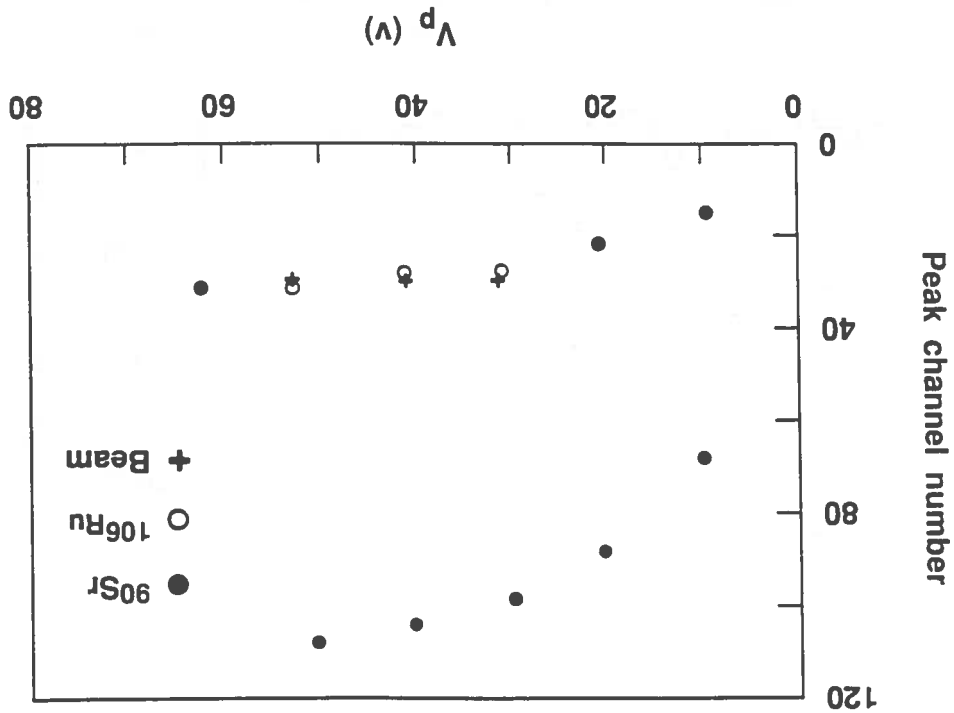


Fig. 8: The peak channel of the pulse-height distribution versus the polarization voltage for  $\beta$  sources and for high energy electron beam.





The first counter available for more complete tests, with a sensitive surface of  $80 \times 10$  mm<sup>2</sup>, will require of the order of  $10^3$  electronic readout channels, and a  $20 \times 20$  cm<sup>2</sup> Si detector plate will require  $2 \times 10^4$  electronic channels.

This can be realized by very large scale integration, which will be carried out by industry and using the valid experience of the SICAPPO Collaboration.

useful one for radiological diagnosis. rays from an energy of 60 keV down to 20 keV. The energy interval 20-60 keV is the Si strip detector with the strip parallel to the beam (fig.12) responds, as predicted, to X- The results from monochromatic X-ray sources are encouraging since they show that a conversion efficiency varies linearly with the depletion thickness.

The rate as a function of  $V_p$  follows a square-root behaviour showing that the the strip water, versus  $V_p$  is shown in fig. 11

The counting rate of the detector exposed to the  $\gamma$ -rays from <sup>241</sup>Am normally striking geometrical configurations (figs. 11 and 12).

The response of the Si strip detector to photons has been measured in two different 7.3 - Exposure to photon-source.

monoenergetic  $\beta$  particles.

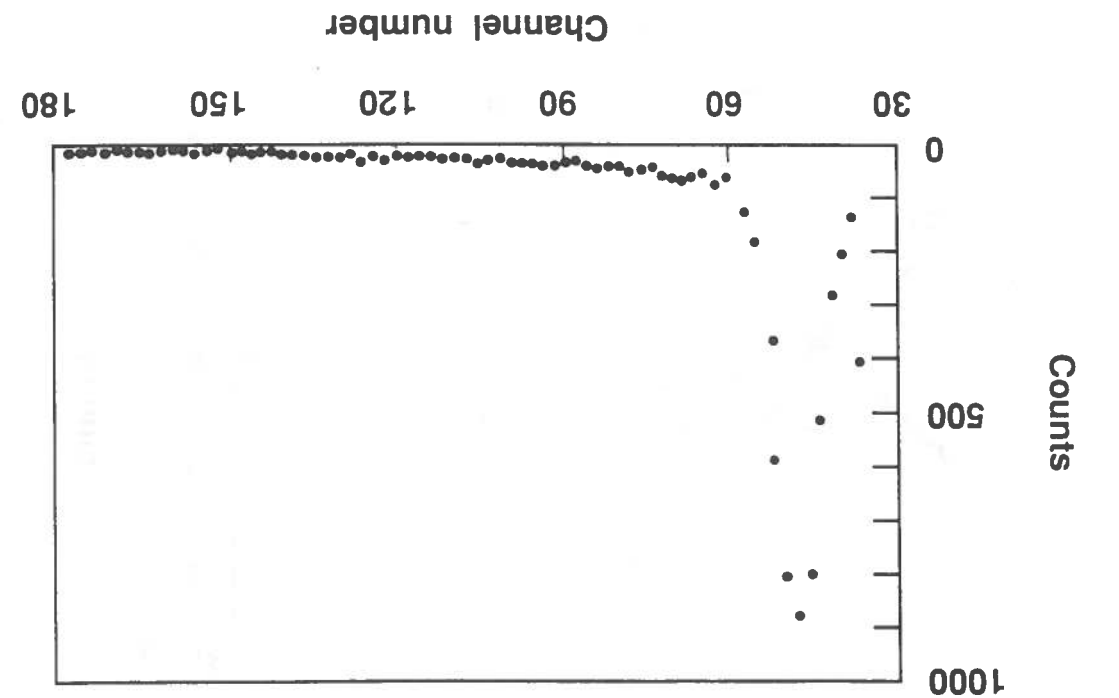


Fig. 10 : The pulse height distribution on a Si strip from test pulses from an Ortec pulser simulating

Fig. 12 : Response of the strip detector to  $\gamma$ -rays incident parallel to the strip as a function of the polarization voltage.

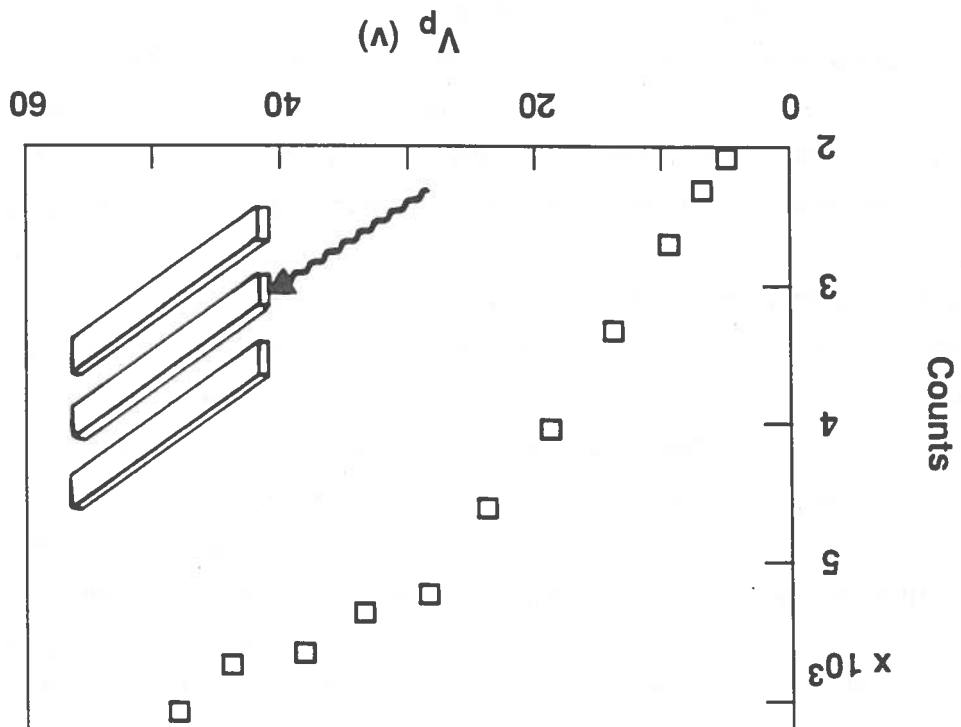
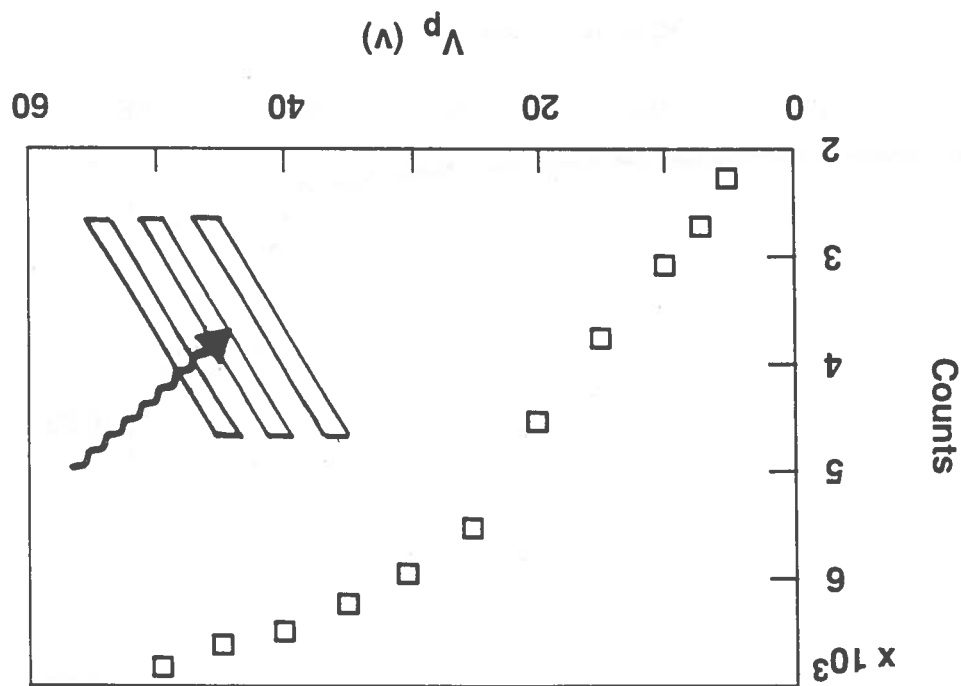


Fig. 11 : Response of the Si strip detector to  $\gamma$ -rays from  $^{241}\text{Am}$  incident normally to the strip as a function of the polarization voltage.



## 8. - Conclusions

We have shown by simple considerations that the use in mammography of the monochromatic X-rays produced from a synchrotron radiation source may present several advantages compared to the X-rays from a conventional radiographic tube. Montecarlo simulations will be needed to confirm these results.

In addition, the use of thin strip detectors which present high efficiency and fast data acquisition capability eliminates several of the shortcomings of the usual photographic films.

The measurements performed with solid state Si strip detectors show that they can be used also as low energy X-ray detectors.

The joint use of synchrotron radiation X-rays and Si strip detectors is a very promising technique that can produce a considerable improvement in mammography.

We feel, than, that it is very important to proceed with the undertaken preliminary project in view of proposing an experimental beamline at the Trieste Synchrotron Radiation Facility.

The program for the next year includes the Montecarlo simulation , the irradiation of a phantom with monochromatic X-rays from an Am source, further measurements with the new silicon strips and the study of an appropriate electronics.

## Appendix - Historical evolution of mammography

At the beginning of mammographic activity, in the early '60s, conventional X-ray equipments and tubes with tungsten anode with 2 mm. focal spot were used. Industrial photographic films were used as detectors, with consequent long exposure times and consistent skin-dose values, about 53 mGy per exposure. The mean dose to the breast was about 16 mGy.

A few years later Charles Gros, from the University of Strasbourg, introduced some relevant changes, supporting the idea that a dedicated mammographic unit was required.

The following fundamental changes were introduced:

- low energy generator;
- X-ray tube with molybdenum anode, which allowed to exploit the emission spectrum of this material;
- 0.7 X 0.7 mm focal spot;
- beryllium window of the tube with a molybdenum filter, which absorbed radiations with energy higher than 30 keV;
- limiting devices for the X-ray beam.

A short time later, another technique, xeromammography<sup>(\*)</sup>, was introduced and turned out to be a good alternative to conventional mammography, because of advantages such as edge enhancement and higher resolution.

At the beginning of the '70s, industrial films were replaced by dedicated film-screen combinations, made with a single-emulsion film very close to the screen.

These systems were capable of lowering the radiation dose (mean dose to the breast of about 6.2 mGy per exposure) and of achieving high contrast and high resolution images, because of reduced exposure times.

Later on, the X-ray tube was changed as well: the focal spot became even smaller ( $0.3 \times 0.4 \text{ mm}^2$ ); most recent tubes have a fine focal spot ( $0.1 \times 0.1 \text{ mm}^2$ ) which allows a radiographic magnification of 1.5-2 times.

---

<sup>(\*)</sup> Xeromammography has been introduced in clinical practice at the end of the '70s and is based on the possibility of image formation by an electrostatic system.

Edge and contrast enhancement are characteristic features of this technique and favoured research and application in this field.

However its widespread use was limited by the inability of finding a satisfactory compromise between image quality and X-ray dose. Presently, xerography seems again a procedure with great capabilities: with not yet commercially available equipments it appears that an image of superior quality (and therefore more information) can be achieved with a dose similar or even inferior to mammography.

Grids enabled better image contrast and resolution by removing scattered radiation: they turned out to be extremely useful when the breast was dense or thicker than 5 cm. In the late '70s rare earth film-screen systems ( $Tb$  activated Gadolinium oxysulfide,  $Tb$  activated Lanthanum oxysulfide) were introduced. They allowed a further reduction of the breast dose (3-4 mGy per exposure) and an improvement of image contrast and resolution. In more recent years some companies introduced films with a very high sensitivity, which is of the utmost importance for achieving a dose reduction, taking into account that mammography is advisable every 1.5-2 years. These films provide an image quality which is close to that of the current films, but with a lower dose (skin dose of 7 mGy and breast dose of 1.2 mGy).

The use of mammographic film-screen systems to image the breast has three major drawbacks: 1) insufficient contrast enhancement for the visualization of subtle tumours and microcalcifications; 2) limited latitude, i.e. in some patients, structures in thin and thick or dense regions of the breast are not clearly visible on the same film; and 3) dose inefficiency, since most mammograms are not limited by the quantum noise.

Digital techniques (i.e. with photosensitive phosphors as detectors) may overcome these problems. Contrast enhancement and edge enhancement allow the extraction of more information than was perceived on the film. Statistical analysis showed both xerography and digitized film superior to film-screen images for the detection of microcalcifications in a phantom study. The difference between xerography and digitized film was not statistically significant. The limit of digital mammography is that film grain noise accounts for at least one-third of the total image noise, and thus limits the degree to which the images can be enhanced.

In conclusion mammographic technology is under continuous development with the aims of lowering the dose and increasing both spatial and contrast resolution. Further improvements will allow the diagnosis of smaller and smaller lesions and the optimal detection of microcalcifications, which may be the only indicator of malignancy. Nowadays more than 90% of breast tumours are recognized: an improvement of this excellent result and the detection of more and more early cancers allow to foresee an earlier therapeutic treatment and thus a higher recovery rate of this neoplasm.

## References

- [1] G.Tromba et. al.: "Coronary angiography at the Trieste Synchrotron Radiation Laboratory", TSRP-IUS-11/86.
- [2] F. Stacul and G. Tromba, "Medical Applications at the Trieste Synchrotron Radiation Laboratory", Proceedings of the Workshop on Scientific and Technological Applications of Synchrotron Radiation, Trieste, May 1987.
- [3] E. Burattini and A. Rindi (editors), Proceedings of the Conference on "Synchrotron Radiation Applications to Digital Angiography", Frascati, May 1987.
- [4] NCRP Report 66 : "Mammography" (1980).
- [5] D.J.Klein: "Experimental and theoretical energy and angular dependencies of scattered radiation in the mammography energy range", Med.Phys.,10 (1983), 664-668.
- [6] M.J.Yaffe et P.C.Johns: "Scattered radiation in diagnostic radiology: magnitudes, effects and methods of reduction", J. Applied Phot. Eng. 9 (1983), 109-129.
- [7] G.Dodd: "Mammography: state of art", Cancer, 53 (1984), 652-657.
- [8] E. Gatti and P.F. Mantredi: "Low noise hybrid pre-amplifiers for high energy physics", Nucl. Instr. Meth. 226 (1984), 142-155.
- [9] P.G. Rancoita and A. Seidman: 'Silicon detectors in calorimetry' Nucl. Instr. Meth. 226 (1984), 369-372.
- [10] E.H.M. Hijne et al.: "A silicon surface barrier microstrip detector designed for high energy physics", Nucl. Instr. Meth. 178 (1980), 331-343.